*Polish Journal of Chemical Technology, 19, **1**, 81—88, 10.1515/pjct-2017-0012*

Sonochemical-assisted magnesium borate synthesis from different boron sources

Meral Yildirim, Azmi Seyhun Kipcak*, Emek Moroydor Derun

Yildiz Technical University, Department of Chemical Engineering, Faculty of Chemical and Metallurgical Engineering, Istanbul, Turkey
**Corresponding author: e-mail: seyhunkipcak@gmail.com; skipcak@yildiz.edu.tr*

In this study, sonochemical-assisted magnesium borate synthesis is studied from different boron sources. Various reaction parameters are successfully applied by a simple and green method. X-ray diffraction (XRD), Fourier transform infrared (FT-IR) and Raman spectroscopies are used to characterize the synthesized magnesium borates on the other hand surface morphologies are investigated by using scanning electron microscope (SEM). The XRD analyses showed that the products were admontite [$MgO(B_2O_3)_3 \cdot 7(H_2O)$] with JCPDS (Joint Committee on Powder Diffraction Standards) no. of 01-076-0540 and mcallisterite [$Mg_2(B_6O_7(OH)_6)_2 \cdot 9(H_2O)$] with JCPDS no. of 01-070-1902. The results that found in the spectroscopic studies were in a good agreement with characteristic magnesium borate bands in both regions of infra-red and visible. According to SEM results, obtained borates were in micro and sub-micro scales. By the use of ultrasonication, reaction yields were found between 84.2 and 97.9%. As a result, it is concluded that the sonochemical approach is a practicable synthesis method to get high efficiency and high crystallinity in the synthesis magnesium borate compounds.

Keywords: magnesium borate, sonochemistry, spectroscopic analysis, ultrasonification, XRD.

INTRODUCTION

In recent years, the green chemistry approach has been become even more important because it aims to increase selectivity of chemical reactions and energy efficiency, to modify the reaction parameters and to minimize the hazardous wastes. Sonochemical synthesis method, which has a conformity with the green chemistry principles, ensures shorter reaction times, enhances reaction yield and provides energy saving[1–3].

In sonochemical-assisted chemical reactions, the interaction of reagents and mass transfer are accelerated with the help of acoustic cavitation which increases surface area for reaction with producing shock waves and causes a strong connection between reactant particles and solution medium[4–9]. In literature, there are many studies that benefit from these advantages of sonochemical synthesis, for producing organic and inorganic compounds such as various nanoparticles (TiO_2, ZnO, Fe_2O_3 etc.), catalysts and biomaterials[10–16].

Being a sub-group of borate compounds, magnesium borates have attractive physical, mechanical and chemical properties that provide them to use in a wide range of industrial applications. Magnesium borates are not only show high heat and corrosion resistance but also have excellent strength, insulation and elasticity specialties. Due to these characteristic features, different types of magnesium borates can be used in various areas, including the thermo-luminescent phosphors, catalysts for hydrocarbon conversions, additives in tunable laser applications, reinforcement in the electronic ceramics, wide band gap semiconductors, reinforcing composites in plastics/aluminum matrixes[17–25].

In literature, magnesium borates are synthesized by several pathways such as hydrothermal[17, 19, 21–23, 26–30], thermal[18, 24], solvothermal synthesis under supercritical conditions[26], phase transformation of double salt of $2MgO \cdot 2B_2O_3 \cdot MgCl_2 \cdot 14H_2O$ [28], chemical vapor deposition and flux assisted thermal conversion methods[20]. On the other hand, the only study about the sonochemical-assisted synthesis of magnesium borate from pure substances is reported by Kipcak et al.[31] which contains production of magnesium borate compounds from MgO and B_2O_3/H_3BO_3, nevertheless, the synthesized product is a mixture of admontite and mcallisterite types of magnesium borates. However, in this study pure admontite production is aimed. Despite the studies about application sonochemistry on the synthesis of different borate compounds[32–35] are accessible in literature, using the sonochemical procedure in the magnesium borate synthesis which presents moderate reaction conditions with short reaction periods has not been studied thoroughly.

In this study, a green, efficient and simple synthesis procedure was applied to obtain magnesium borates from different boron sources under ultrasonic irradiation. Besides different boron sources, effects of various reaction times (5–20 min) and reaction temperatures (60–100°C) were investigated. In addition to reaction yield and boron oxide (B_2O_3) calculations; chemical, morphological and spectral properties of produced magnesium borates were compared to find out the optimum reaction conditions for sonochemical-assisted magnesium borate production.

EXPERIMENTAL STUDIES

Raw materials

Magnesium chloride hexahydrate ($MgCl_2 \cdot 6H_2O$) with a purity of 99%, borax ($Na_2B_4O_7 \cdot 10H_2O$), tincalconite ($Na_2B_4O_7 \cdot 5H_2O$) and boric acid (H_3BO_3) with the purities of 99.9% and boron oxide (B_2O_3) with the purity of 98%, were used as the precursor materials for the synthesis. Magnesium chloride hexahydrate ($MgCl_2 \cdot 6H_2O$) was obtained from Merck chemicals (Merck KgaA, Darmstadt, Germany) (CAS No: 7791-18-6). The boron sources were procured from Bandırma Boron Works (Eti Maden, Balıkesir, Turkey). Before the synthesis, boron sources were ground by Retsch RM 100 (Retsch GmbH & Co KG, Haan, Germany) and sieved through

by Fritsch analysette 3 Spartan pulverisette 0 vibratory sieve-shaker (Fritsch, Idar-Oberstein, Germany) to access a particle size of 75 μm. In pursuit of preparation, characterization of raw materials was done by PANalytical Xpert Pro (PANalytical B.V., Almelo, The Netherlands) X-ray diffractometer (XRD) with the parameters of 45 kV and 40 mA (Cu- Kα tube, λ = 0.15318 nm).

Sonochemical-assisted synthesis

Sonochemical-assisted synthesis of magnesium borate compounds was carried out by the hydrothermal procedure by direct-immersion of Bandelin Sonopuls HD 2070 ultrasonic homogenizers (Bandelin electronic GmbH & Co. KG, Berlin, Germany) that use the operation frequency of 20 kHz. In the experiments, 1:6 magnesium to boron (Mg:B) molar ratio was used, which was determined from preliminary synthesis[29], magnesium and boron sources were reacted with ultrasonic irradiation in a batch type reactor filled with distilled water obtained from GFL 2004 (Gesellschaft für Labortechnik, Burgwedel, Germany) water purification system.

In the present study, four sets of experiments were applied, which are coded as Mc-Bx-B (Set 1), Mc-Bx-H (Set 2), Mc-T-B (Set 3), Mc-T-H (Set 4), where the abbreviations symbolize the raw materials as "Mc" for $MgCl_2 \cdot 6H_2O$, "Bx" for $Na_2B_4O_7 \cdot 10H_2O$, "T" for $Na_2B_4O_7 \cdot 5H_2O$, "B" for B_2O_3 and "H" for H_3BO_3.

To investigate the influence of reaction temperature and sonification time on the products, the reaction temperature was varied between 60–100°C and sonification time was varied between 5–20 min. At the end of determined sonification time, the reaction slurry was placed in an Ecocell LSIS-B2V/EC55 model incubator (MMM Medcenter Einrichtungen GmbH, Planegg, Germany) maintained at 40°C. In the incubator the magnesium borates were crystallized and the excess water was evaporated. In the synthesis, the usage of sodium borates leads to form sodium chloride (NaCl) as by-product, so on the purpose of removing that by-product and excess or unreacted amount of H_3BO_3, the products were washed with ethanol (96%) obtained from Merck chemicals (Merck KgaA, Darmstadt, Germany) (CAS No: 64-17-5) and filtered through chm F2044 grade (Ashless, slow filter speed) 90 mm blue ribbon filter paper (Chmlab, Barcelona, Spain). Then the filter cake was dried in the incubator again at 40°C. The reaction scheme of the entire production is given in Figure 1.

Characterization studies of synthesized magnesium borates

XRD, Fourier transform infrared spectroscopy (FT-IR), Raman spectroscopy and scanning electron microscopy (SEM) were applied to characterize the synthesized products. Phase composition of products was determined by XRD in the pattern range of 7–60°. The infrared absorption spectra of the products in the wavenumber range of 1800–650 cm^{-1} were obtained by PerkinElmer Spectrum One FT-IR (PerkinElmer, MA, USA). Raman spectra were obtained between the ranges of 1800–250 cm^{-1} by using Perkin Elmer Raman Station 400F (PerkinElmer, CT, USA). The spectroscopic ranges were determined by through previous studies that the characteristic peaks of borate compounds, which were observed in the range of 500–1500 cm^{-1} [18, 36].

The morphological properties and particle sizes of magnesium borates were investigated by CamScan Apollo 300 Field-Emission SEM (CamScan, Oxford, United Kingdom) working at 20 kV. Backscattering electron detector (BEI) was used in the morphological studies. The SEM images of products were magnified as 10 000 times.

In terms of economy, the commercial value of borate compounds is assessed depending on their B_2O_3 content. Therefore, B_2O_3 percentage of synthesized compounds were calculated by the method given by the studies in literature[30, 31, 36].

Yield analysis was conducted with choosing $MgCl_2 \cdot 6H_2O$ as a key component of the procedure of given by Derun et al.[37]. The experiments were carried out three repetitions and the average yield and standard deviation values were calculated. For biphasic products,

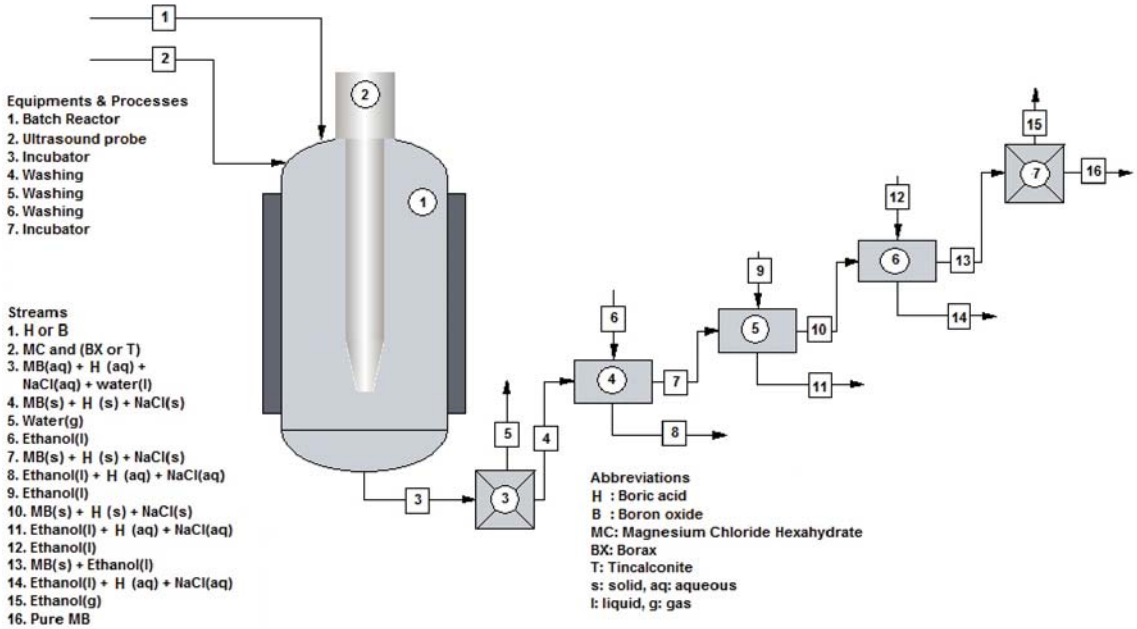

Figure 1. Reaction scheme

the yield calculations were applied according to the phase which's molecular weight is higher.

The overall yields, Y_D, is calculated by dividing the number of moles of product at the final stage, N_D, by the number of consuming moles of the key reactant, A. The consuming numbers of moles of reactant, A, is calculated by using the initial (N_{A0}) and the final (N_A) numbers of moles reactant with the Eq. 1 [37, 38].

$$Y_D = \frac{N_D}{N_{A0} - N_A} \quad (1)$$

RESULTS AND DISCUSSION

Results of the raw material characterization

According to the XRD results of the raw materials, the boron sources were identified as sassolite (H_3BO_3) with JCPDS (Joint Committee on Powder Diffraction Standards) no. of 01-073-2158, boron oxide (B_2O_3) with JCPDS no. of 00-006-0297 (B_2O_3) and 01-088-2485 (B_2O), tincalconite ($Na_2B_4O_7 \cdot 5H_2O$) with JCPDS no. of 01-079-1529 and borax ($Na_2B_4O_7 \cdot 10H_2O$) with JCPDS no. of 01-075-1078, respectively. The XRD pattern of magnesium source was attuned to bischofite ($MgCl_2 \cdot 6H_2O$) with JCPDS no. of 01-077-1268.

XRD results of the synthesized magnesium borates

XRD scores of synthesized magnesium borates obtained from different sources of boron compounds are given in Table 1. From the results, in all of the four sets, the major component was found as "admontite" [$MgO(B_2O_3)_3 \cdot 7(H_2O)$] type of a magnesium borate mineral with JCPDS no. of 01-076-0540. In 9 experiments, diphase production was observed and besides admontite, "mcallisterite" [$Mg_2(B_6O_7(OH)_6)_2 \cdot 9(H_2O)$] type of a magnesium borate mineral with the JCPDS no. of 01-070-1902 was formed, among the 48 experiments.

In the set of "Mc-Bx-B", the highest and the lowest admontite XRD scores were observed at the conditions of 80°C – 5 min and 80°C – 20 min, respectively. Since the XRD scores were close to each other it can be said that the admontite crystal formation was not affected by the reaction temperature and reaction time much. In the set of "Mc-Bx-H" the highest and the lowest admontite XRD scores were observed at the at the condition of 60°C – 20 min and 100°C – 15 min, respectively. In this set the XRD scores were lower than the set of "Mc-Bx-B". In general, higher XRD scores were obtained at the reaction temperature of 60°C and were decreased with increasing reaction temperature. In the set of "Mc-T-B", the highest and the lowest admontite XRD scores were observed at the at the condition of 100°C – 10 min and 60°C – 5 min (also 80°C – 10 min), respectively. In this set of experiments, higher XRD scores were obtained that the sets of "Mc-Bx-B" and "Mc-Bx-H" and these scores were increased with increasing reaction temperature. In the last set of "Mc-Bx-H" the highest and the lowest admontite XRD scores are observed at the condition of 80°C – 20 min and 100°C – 15 min, respectively. Likewise, in the set of "Mc-T-B", higher XRD scores were obtained at the sets of "Mc-Bx-B" and "Mc-Bx-H". For the comparison of the sets of "Mc-Bx-B" and "Mc-Bx-H", on the set of "Mc-Bx-H", higher XRD scores of admontite were seen for the temperature of 80°C reaction time. Comparing all of the set admontite XRD scores, 60°C reaction temperature and 20 min of reaction time can be selected as the optimum synthesis conditions for a green chemical approach (low reaction temperature and low reaction time). These optimum products' XRD patterns are given in Figure 2. From Figure 2, it is seen that these products have ten major characteristic peaks (h k l, d [Å]) at approximately 7.4° (1 0 0, 11.93 Å), 12.1° (0 1 1, 7.33 Å), 15.57° (1 1 1, 5.69 Å), 15.7° (–1 0 2, 35.62 Å), 16.6° (0 0 2, 5.33 Å), 16.8° (–2 1 1, 5.26 Å), 18.2° (–2 0 2, 4.87 Å), 22.7° (–2 2 1, 3.90 Å), 28.9° (–4 0 2, 3.08 Å) and 33.65° (1 3 2, 3.90 Å). Detailed crystallization data of admontite was given in the study of Kipcak et al.[29].

Comparison with the literature, the ultrasonication ensures more crystalline magnesium borate powders produced in previous studies even for 5 minutes of reaction at 60°C [29, 31, 36].

FT-IR and Raman spectroscopy of the synthesized magnesium borates

FT-IR and Raman spectra of the selected magnesium borate minerals are presented in Figure 3 and Figure 4, respectively. According to FT-IR spectra, two absorption peaks were observed at 1420 cm^{-1} and 1345 cm^{-1}. The peaks were arisen because of the asymmetric stretching of the three-coordinate boron to oxygen bands [$\nu_{as}(B_{(3)}\text{-}O)$]. The peak at 1234 cm^{-1} might be due to bending of boron-oxygen-hydrogen [δ(B-O-H)] and the peaks which were observed at 1087 cm^{-1} and 1021 cm^{-1} were related

Table 1. XRD scores of the synthesized magnesium borates for different sets

Reaction temperature [°C]	Reaction time [min]	Mc–Bx–B		Mc–Bx–H		Mc–T–B		Mc–T–H	
		▲	■	▲	■	▲	■	▲	■
60	5	58	–	54	–	65	–	70	–
	10	60	–	60	–	67	–	65	–
	15	59	–	61	–	73	–	69	–
	20	**64**	**–**	**66**	**–**	**73**	**–**	**71**	–
80	5	68	–	62	–	68	38	70	55
	10	61	–	60	–	65	–	74	34
	15	65	–	59	–	73	–	76	–
	20	55	–	64	–	72	–	78	–
100	5	63	–	59	–	74	35	74	–
	10	62	–	53	38	75	–	67	–
	15	62	–	51	49	72	–	58	57
	20	64	17	59	–	73	–	67	56

▲: Admontite, ■: Mcallisterite.

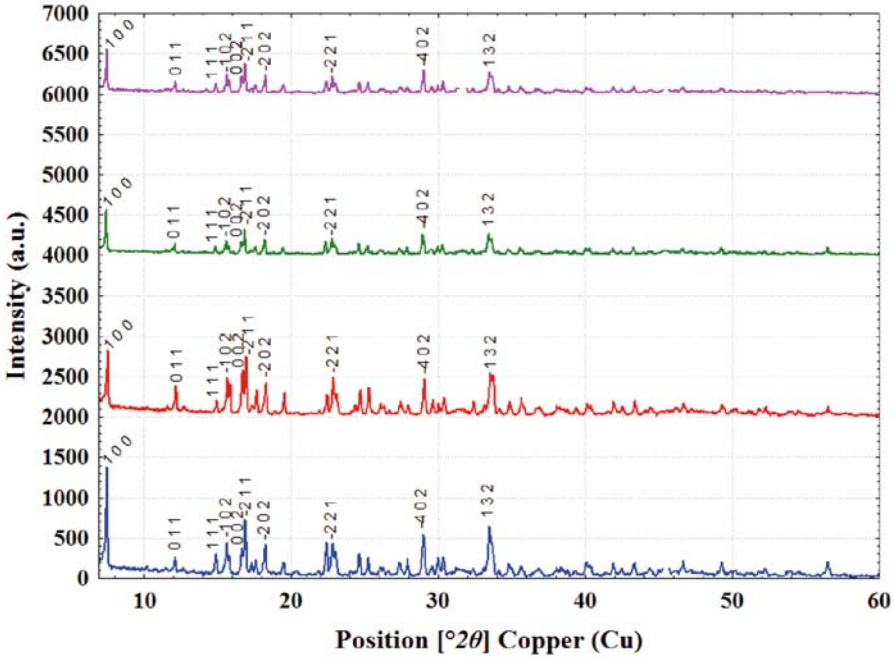

Figure 2. XRD patterns of the synthesized optimum magnesium borates

to the asymmetric stretching of four-coordinate boron to oxygen bands [$\nu_{as}(B_{(4)}\text{-}O)$]. The presence of IR peaks between 995–953 cm^{-1} and 897 cm^{-1} revealed the symmetric stretching of the three-coordinate boron to oxygen bands [$\nu_{s}(B_{(3)}\text{-}O)$]. Also, the peaks below 858 cm^{-1} were due to the symmetric stretching of the four-coordinate boron to oxygen bands [$\nu_{s}(B_{(4)}\text{-}O)$][31, 37].

In the Raman spectra, the band around 962 cm^{-1} showed $\nu_{as}(B_{(4)}\text{-}O)$. The peaks which observed at approximately 636 cm^{-1} is the characteristic bands of three six-member rings of one BO_3 planar triangle and two BO_4 tetrahedrons ($\nu_p[B_6O_7(OH)_6]^{2-}$ / $\nu_p[B_3O_3(OH)_4]^-$). The peaks at 427 and 303 cm^{-1} could correspond to bending of four-coordinate boron to oxygen bands $\delta(B_{(4)}\text{-}O)$[31, 37].

Both FT-IR and Raman spectra of products showed characteristic absorption and scattering peaks of magnesium borates, respectively[29, 31, 37].

B_2O_3 contents of the synthesized minerals

Table 2 shows the B_2O_3 content of the synthesized magnesium borate minerals for all reaction times and reaction temperatures. For reaction sets of 1, 2, 3 and 4 the B_2O_3 contents were determined between 55.93—41.87%, 54.65–37.04%, 52.04–45.86%, 55.47–43.79%, respectively. Obtained B_2O_3 results are in conformity with the literature[37, 39]. Where the theoretical B_2O_3 contents of the mcallisterite and admontite are given in the literature as 54.35% and 55.66%, respectively.

Surface morphology and particle size of the synthesized magnesium borate compounds

To find out the effect of different reactants, reaction temperatures, and reaction times on the surface morphology of the produced magnesium borates, SEM analyses were applied to the products. The surface morphologies and particle size ranges of optimum products are shown in Figure 5.

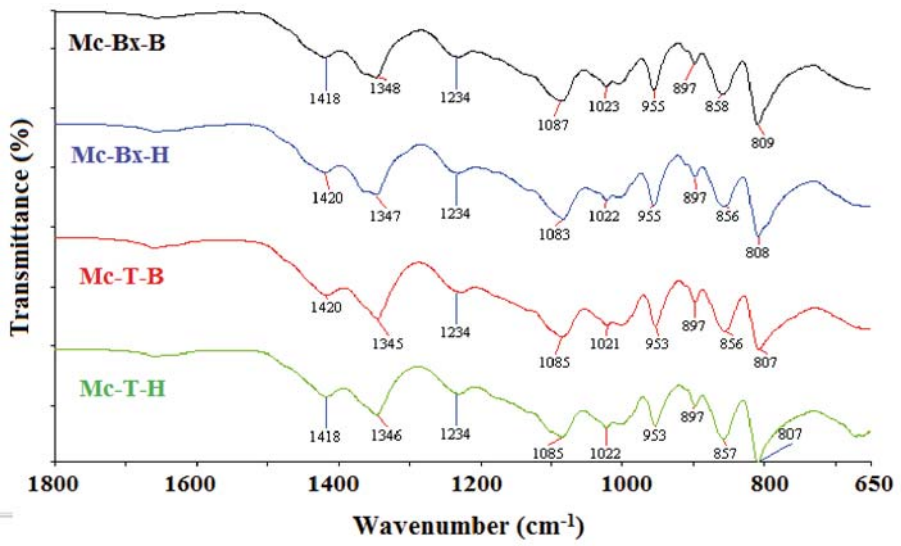

Figure 3. FT-IR spectra of optimum magnesium borates

Table 2. B_2O_3 contents of the synthesized magnesium borate compounds

Reaction temperature [°C]	Reaction time [min]	B_2O_3 [%]			
		Set 1	Set 2	Set 3	Set 4
60	5	44.59 ±1.75	51.21 ±1.87	47.43 ±2.56	45.61 ±3.34
	10	53.33 ±0.79	55.93 ±1.37	48.86 ±0.42	43.79 ±2.25
	15	51.65 ±0.50	52.54 ±0.63	52.04 ±1.35	50.19 ±1.25
	20	41.87 ±1.82	54.65 ±3.16	45.90 ±3.14	51.08 ±0.10
80	5	50.27 ±2.29	54.27 ±1.59	47.64 ±2.92	55.47 ±0.99
	10	54.04 ±1.37	43.48 ±2.28	47.53 ±3.34	47.71 ±4.55
	15	54.42 ±2.00	37.04 ±2.28	49.89 ±3.14	54.48 ±4.70
	20	54.30 ±0.67	43.48 ±2.28	48.89 ±4.76	49.79 ±3.08
100	5	54.27 ±2.04	53.92 ±1.79	45.86 ±2.25	45.61 ±3.34
	10	54.01 ±0.25	53.18 ±0.42	49.30 ±6.06	48.60 ±4.55
	15	51.89 ±1.08	54.24 ±1.83	51.21 ±6.59	54.55 ±2.72
	20	49.92 ±2.73	54.65 ±3.16	45.86 ±2.25	48.49 ±2.30

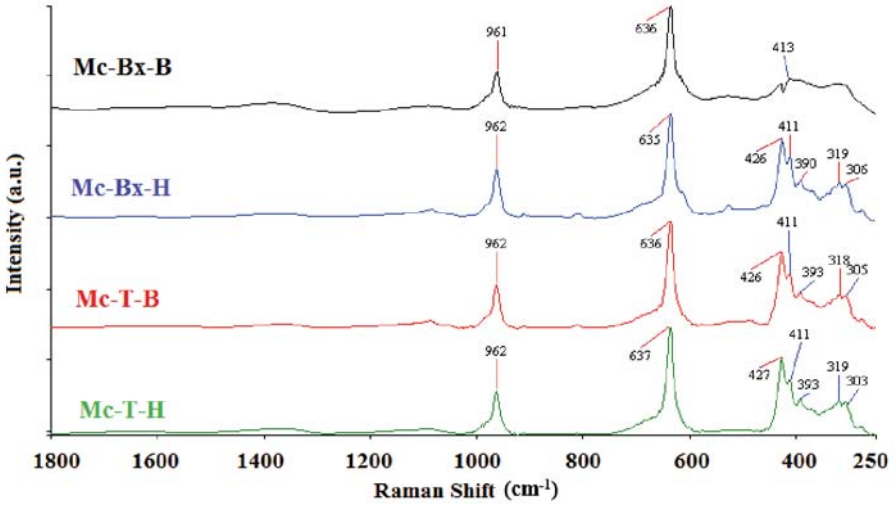

Figure 4. Raman spectra of selected magnesium borates

According to SEM results, the particle size of synthesized minerals is in micro and sub-micro scale. For Set 1, the particle size of products changed between 1.18 μm – 228.87 nm and the acquired particles had smooth, multangular layer with smaller pieces. Also irregularities in particle texture with sharp edges could be observed in Set 1. In the reactions that borax and boron oxide used as boron source (Set 2), the products showed non-

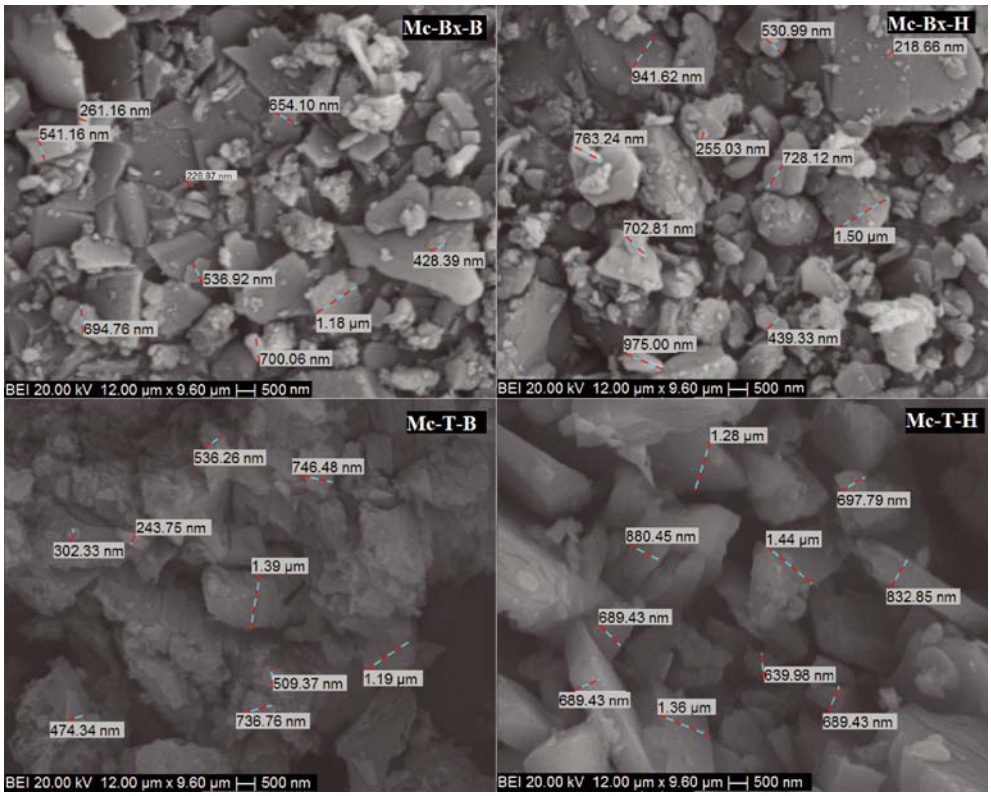

Figure 5. SEM morphologies of the selected magnesium borates

uniform particle size distribution which varied between 1.50 μm – 218.66 nm. For Set 3 and Set 4, in which tincalconite was used, the particle size changed between 1.39 μm – 243.75 nm and 1.44 μm – 639.98 nm. Also it was seen that when tincalconite used as a boron source, the particle sizes were increased because of the increase of the agglomeration. For Set 3, conglomerated structures could be noticed which was because of summing up of small particles.

Produced magnesium borate powders had smaller average particle size contrary to previous studies[29, 31, 37] since the ultrasonic probe leads more homogeneous stirring in the reaction medium.

Yield calculation of synthesized magnesium borates

Reaction yields of magnesium borates are presented in Figure 6a for Set 1 and Set 2, in Figure 6b for Set 3 and Set 4. According to the results, for all reaction sets the highest reaction yields were obtained at increasing reaction time and reaction temperature. When each reaction set was scrutinized in detail, it is seen that the yield of reactions in which H_3BO_3 was used is found higher.

The calculated reaction yields were between 85.8–94.6%, 87.2–97.9%, 84.2–94.1%, 86.5–96.1% for Set 1, Set 2, Set 3 and Set 4, respectively. The highest yield was observed in the experiment of Set 2 which was taking place at 100°C during 20 min of reaction time.

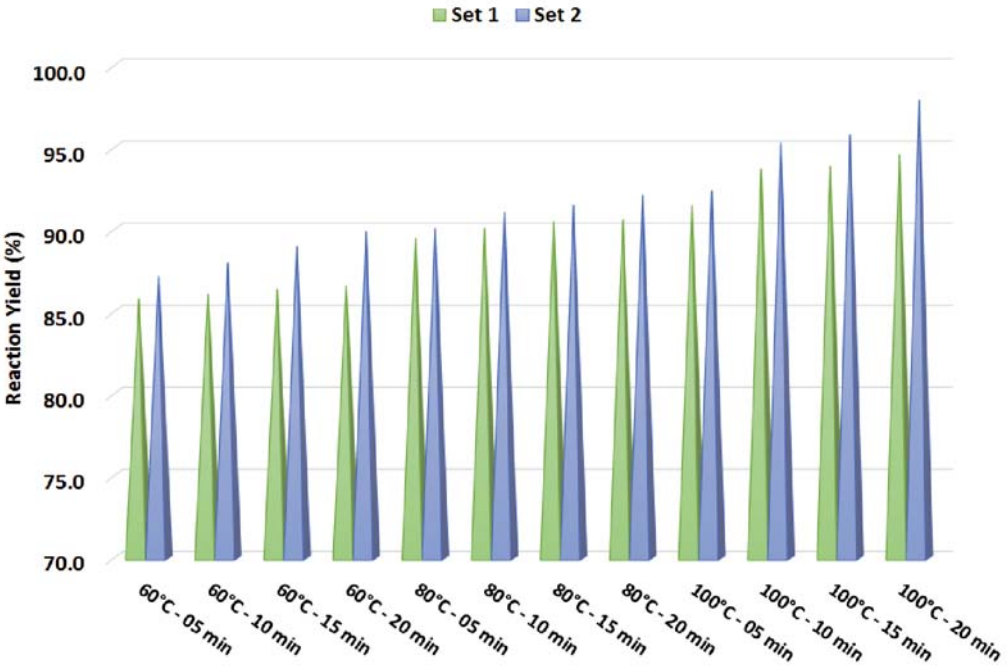

Figure 6a. Reaction yields of Set 1 and Set 2

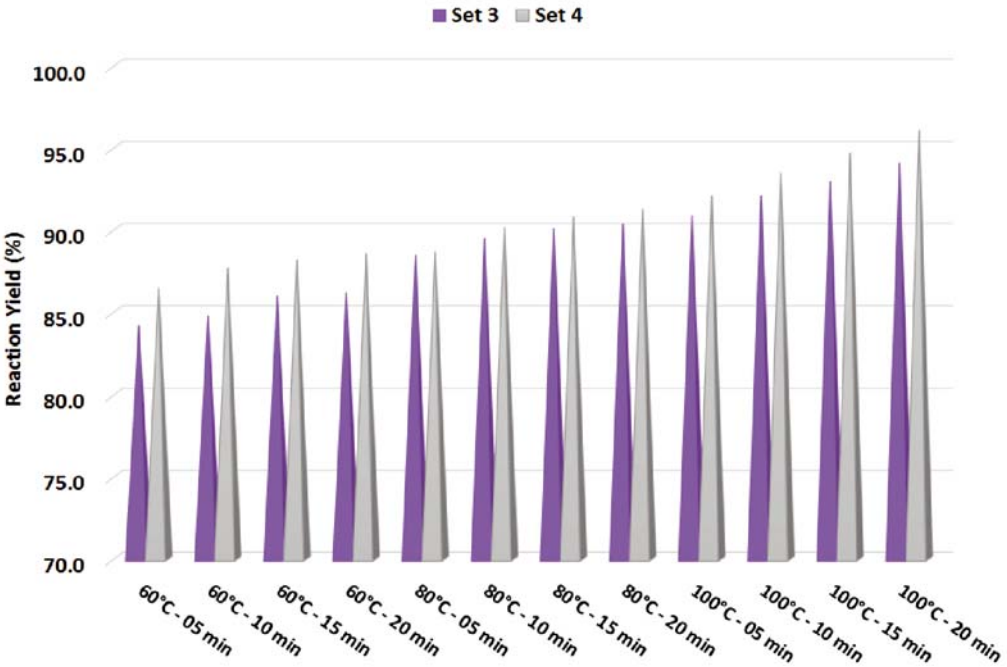

Figure 6b. Reaction yields of Set 3 and Set 4

CONCLUSIONS

In this study, a novel and green method was developed to synthesis magnesium borate compounds with high crystallinity from different boron sources by ultrasonication. XRD results showed that admontite [$MgO(B_2O_3)_3 \cdot 7(H_2O)$] and mcallisterite [$Mg_2(B_6O_7(OH)_6)_2 \cdot 9(H_2O)$] were produced during study where the main phase was admontite in the most of the experiments. The reaction yields of experiments changed between 84.2–97.9%.

The study indicates that even at 60°C and 5 min of reaction, high crystalline magnesium borate compounds can be produced. Therefore, in comparison with our previous study[29], the usage ultrasonic synthesis method provides lower reaction times and reaction temperatures, which ensures energy saving, simple and green obtainment of desired compounds.

ACKNOWLEDGMENTS

This research was supported by the Yildiz Technical University Scientific Research Projects Coordination Department, Project Number 2013-07-01-GEP04.

LITERATURE CITED

1. Mason, T.J. (2003). Sonochemistry and Sonoprocessing: The link, the trends and (probably) the future. Ultrason. Sonochem. 10, 175–179. DOI: 10.1016/S1350-4177(03)00086-5.
2. Mason, T.J. (2007). Sonochemistry and the environment – Providing a "Green" link between chemistry, physics and engineering. Ultrason. Sonochem. 14, 476–483. DOI: 10.1016/j.ultsonch.2006.10.008.
3. Cintas, P. & Luche, J.L. (1999). The sonochemical approach. Green Chem. 1, 115–125. DOI: 10.1039/A900593E.
4. Gedanken, A. (2004). Using sonochemistry for the fabrication of nanomaterials. Ultrason. Sonochem. 11, 47–55. DOI: 10.1016/j.ultsonch.2004.01.037.
5. Bang, J.H. & Suslick, K.S. (2010). Applications of ultrasound to the synthesis of nanostructured materials. Adv. Mater. 22, 1039–1059. DOI: 10.1002/adma.200904093.
6. Kurikka, K.V.P.M., Ulman, A., Yan, X., Yang, N., Estournes, C., White, H. & Rafailovich, M. (2001). Sonochemical synthesis of functionalized amorphous iron oxide nanoparticles. Langmuir 17, 5093–5097. DOI: 10.1021/la010421+.
7. Kumar, B., Smita, K., Cumbal, L., Debut, A. & Pathak, R.N. (2014). Sonochemical synthesis of silver nanoparticles using starch: A comparison. Bioinorg. Chem. Appl. DOI: 10.1155/2014/784268.
8. Mettin, R. Cairós, C. & Troia, A. (2015). Sonochemistry and bubble dynamics. Ultrason. Sonochem. 25, 24–30. DOI: 10.1016/j.ultsonch.2014.08.015.
9. Suslick, K.S. & Price, G.J. (1999). Applications of ultrasound to materials chemistry. Annu. Rev. Mater. Sci. 29, 295–326.
10. Zak, A.K., Majid, W.H., Wang, H.Z., Yousefi, R., Golsheikh, A.M. & Ren, Z.F. (2013). Sonochemical synthesis of hierarchical ZnO nanostructures. Ultrason. Sonochem. 20, 395–400. DOI: 10.1016/j.ultsonch.2012.07.001.
11. Kim, W., Choi, D. & Kim, S. (2010). Sonochemical synthesis of zeolite: A from metakaolinite in NaOH solution. Mater. Trans. 9, 1694–1698. DOI: 10.2320/matertrans.M2010191.
12. Safaei-Ghomi, J. & Akbarzadeh, Z. (2015). Sonochemically Synthesis of arylethynyl linked triarylamines catalyzed by CuI nanoparticles: A rapid and green procedure for sonogashira coupling. Ultrason. Sonochem. 22, 365–370. DOI: 10.1016/j.ultsonch.2014.05.016.
13. Sadr, M.H. & Nabipour, H. (2013). Synthesis and identification of carvedilol nanoparticles by ultrasound method. J. Nanostruct. Chem. 3: 26. DOI: 10.1186/2193-8865-3-26.
14. Hernández-Perez, I., Maubert, A.M., Rendón, L., Santiago, P., Herrera-Hernández, H., Díaz-Barriga Arceo, L., Garibay Febles, V., Palacios González, E. & González-Reyes, L. (2012). Ultrasonic Synthesis: structural, optical and electrical correlation of TiO_2 nanoparticles. Int. J. Electrochem. Sci. 7, 8832–8847.
15. Coskuner, B., Kanturk Figen, A. & Piskin, S. (2014). Sonochemical approach to synthesis of Co-B catalysts and hydrolysis of alkaline $NaBH_4$ solutions. J. Chem. Article ID 185957. DOI: 10.1155/2014/185957.
16. Hu, X., Lu, Q., Sun, L., Cebe, P., Wang, X., Zhang, X. & Kaplan, D.L. (2010). Biomaterials from ultrasonication-induced silk fibroin-hyaluronic acid hydrogels. Biomacromolecules 11, 3178–3188. DOI: 10.1021/bm1010504.
17. Dou, L., Zhong, J. & Wang, H. (2010). Preparation and characterization of magnesium borate for special glass. Phys. Scr. T139:2010: 014010. DOI: 10.1088/0031-8949/2010/T139/014010.
18. Li, S., Xu, D., Shen, H., Zhou, J. & Fan, Y. (2012). Synthesis and Raman properties of magnesium borate micro/nanorods. Mater. Res. Bull. 47, 3650–3653. DOI: 10.1016/j.materresbull.2012.06.046.
19. Kumari, L., Li, W.Z., Kulkarni, S., Wu, K.H., Chen, W., Wang, C., Vannoy, C.H. & Leblanc, R.M. (2010). Effect of surfactants on the structure and morphology of magnesium borate hydroxide nanowhiskers synthesized by hydrothermal route. Nanoscale Res. Lett. 5, 149–157. DOI: 10.1007/s11671-009-9457-9.
20. Zhu, W., Zhang, Q., Xiang, L., Wei, F., Sun, X., Piao, X. & Zhu, S. (2008). Flux-assisted thermal conversion route to pore-free high crystallinity magnesium borate nanowhiskers at a relatively low temperature. Cryst. Growth Des. 8, 2938–2945. DOI: 10.1021/cg800050u.
21. Zhu, W., Xiang, L., He, T. & Zhu, S. (2006). Hydrothermal synthesis and characterization of magnesium borate hydroxide nanowhiskers. Chem. Lett. 35, 1158–1159. DOI: 10.1246/cl.2006.1158.
22. Zhu, W., Zhang, X., Xiang, L. & Zhu, S. (2009). Hydrothermal formation of the head-to-head coalesced szaibelyite $MgBO_2(OH)$ nanowires. Nanoscale Res. Lett. 4, 724–731. DOI: 10.1007/s11671-009-9306-x.
23. Zhu, W., Li, G., Zhang, Q., Xiang, L. & Zhu, S. (2010). Hydrothermal mass production of $MgBO_2(OH)$ nanowhiskers and subsequent thermal conversion to $Mg_2B_2O_5$ nanorods for biaxially oriented polypropylene resins reinforcement. Powder Technol. 203, 265–271. DOI: 10.1016/j.powtec.2010.05.017.
24. Elssfah, E.M., Elsanousi, A., Zhang, J., Song, H.S. & Tang, C. (2007). Synthesis of magnesium borate nanorods. Mater. Lett. 61, 4358–4361. DOI: 10.1016/j.matlet.2007.02.002.
25. Li, Y., Fan, Z., Lu, J.G. & Chang, R.P.H. (2004). Synthesis of magnesium borate ($Mg_2B_2O_5$) nanowires by chemical vapor deposition method. Chem. Mater. 16, 2512–2514. DOI: 10.1021/cm0496366.
26. Xu, B.S., Li, T.B., Zhang, Y., Zhang, Z.X., Liu, X.G. & Zhao, J.F. (2008). New synthetic route and characterization of magnesium borate nanorods. Cryst. Growth Des. 8, 1218–1222. DOI: 10.1021/cg700690g.
27. Wang, G., Wang, K., Hou, J., Wang, Y. & Kong, C. (2011). Preparation of magnesium borate nanomaterials by hydrothermal route. Adv. Mater Res. 320, 642–646. DOI: 10.4028/www.scientific.net/AMR.320.642.
28. Zhihong, L. & Mancheng, H. (2004). New synthetic method and thermochemistry of szaibelyite. Thermochim. Acta 411, 27–29. DOI: 10.1016/j.tca.2003.07.009.
29. Kipcak, A.S., Yildirim, M., Aydin Yuksel, S., Moroydor Derun, E. & Piskin, S. (2014). The synthesis and physical properties of magnesium borate mineral of admontite synthesized from sodium borates. Adv. Mater. Sci. Eng. ID 819745. DOI: 10.1155/2014/819745.

30. Moroydor Derun, E. & Senberber, F.T. (2014). Characterization and thermal dehydration kinetics of highly crystalline mcallisterite, synthesized at low temperatures. Sci. World J. ID 985185. DOI: 10.1155/2014/985185.
31. Kipcak, A.S., Moroydor Derun, E. & Piskin, S. (2014). Synthesis and characterization of magnesium borate minerals of admontite and obtained via ultrasonic mixing of magnesium oxide and various sources of boron: A novel method. Turk. J. Chem. 38, 792–805. DOI: 10.3906/kim-1307-61.
32. Taylan, N., Gurbuz, H. & Bulutcu, A.N. (2007). Effects of ultrasound on the reaction step of boric acid production process from colemanite. Ultrason. Sonochem. 14, 633–638. DOI: 10.1016/j.ultsonch.2006.11.001.
33. Aksener, E., Kanturk Figen, A. & Piskin, S. (2014). Synthesis of nanometric β-Barium metaborate powder from different borate solutions by ultrasound-assisted precipitation. Res. Chem. Intermed. 40, 2103–2117. DOI: 10.1007/s11164-013-1106-3.
34. Gayathri Devi, A.V., Rajendran, V., Jeyasubramanian, K., Suresh Kumar, N. & Abdel-Hameed, S.A.M. (2006). Ultrasonic investigation on nanocrystalline barium borate (BBO) glass ceramics. Synth. React. Inorg. Me. 36, 215–219.
35. Yilmaz, M.S., Kanturk Figen, A. & Piskin, S. (2012). Production of sodium metaborate tetrahydrate ($NaB(OH)_4 \cdot 2H_2O$) using ultrasonic irradiation. Powder Technol. 215–216, 166–173. DOI: 10.1016/j.powtec.2011.09.043.
36. Yongzhong, J., Shiyang, G., Shuping, X. & Jun, L. (2000). FT-IR spectroscopy of supersaturated aqueous solutions of magnesium borate. Spectrochim. Acta A. 56, 1291–1297. DOI: 10.1016/j.saa.2004.02.027.
37. Moroydor Derun, E., Kipcak A.S., Senberber, F.T. & Sari Yilmaz, M. (2015). Characterization and thermal dehydration kinetics of admontite mineral hydrothermally synthesized from magnesium oxide and boric acid precursor. Res. Chem. Intermed. 41, 853–866. DOI: 10.1007/s11164-013-1237-6.
38. Fogler, H.S., Element of Chemical Reaction Engineering, Fifth ed., Prentice-Hall, Indiana, 2016.
39. Anthony, J.W., Bideaux, R.A., Bladh, K.W., Nichols & M.C. Mcallisterite- Handbook of Minerology, First ed., Mineral Data Publishing, Virginia, 2003.